Electronic Supplementary Material (ESI) for Analyst

Integrated label-free silicon nanowire sensor arrays for (bio)chemical analysis

Arpita De, Jan van Nieuwkasteele, Edwin T. Carlen*, Albert van den Berg

BIOS Lab on a Chip Group, Mesa+ Institute for Nanotechnology, University of Twente, Postbus 217, 7500 AE Enschede, The Netherlands

*Corresponding author: Dr. Edwin Carlen, University of Twente, MESA+ Institute for Nanotechnology, P.O. Box 217, 7500 AE Enschede, The Netherlands; Tel:+31 (0)53 489 5399; Fax: +31 (0)53 489 3595; Email: e.t.carlen@utwente.nl

Sample injection design and testing protocol

A typical sample injection protocol using the microfluidic autosampler system is described. A sample plug injection from SR_1 is injected into the microfluidic flow-cell with buffer from SR_2. Figure S1 shows the different valve positions that are automatically set as switch position A or B during the injection procedure.

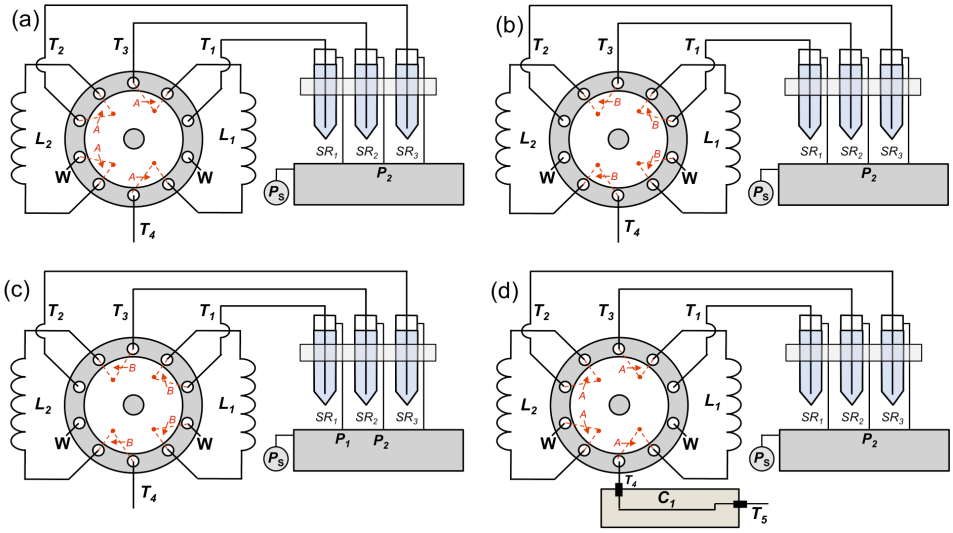

Fig. S1 Automated sample injector protocol.

The protocol for the loading and injection of a single sample is described below:

Step 1 (Fig. S1a and Fig. S1b): System purge (microfluidic flow-cell not connected to T_4):

1. Purge sample loop L_1 with buffer (SR_2, P_2=1 bar; T_3+L_1+T_4; Fig. S1a, switch pos. A)
2. Purge sample loop L_2 with buffer (SR_2, P_2=1 bar; T_3+L_2+T_4; Fig. S1b, switch pos. B)

Step 2 (Fig. S1c, switch pos. B): Load sample 1 to loop L_1:

1. Load sample loop L_1 with sample 1 (SR_1, P_1=1 bar; T_1+L_1 to waste W)
2. Stop when sample appear at waste W outlet

Step 3 (Fig. S1d, switch pos. A): Injection of sample 1 (SR_1):

1. Connect T_4 to microfluidic flow-cell
2. Continue injecting buffer (SR_2, P_3=1 bar) through sample loop L_2 and microfluidic flow-cell (T_3+L_2+T_4+C_1+T_5) using maximum drive pressure, i.e. P_2=1 bar
3. When sensor output is stable inject sample 1 (SR_2, P_2;T_3+L_1+T_4+C_1+T_5)

The tubing lengths and diameters (T_3, T_4 and T_5) are determined by the range of the regulated pressure source P_2 and desired sample flow rate Q. The total equivalent hydraulic resistance R_{hyd} and the volumetric flow rate Q can be estimated with $Q=\Delta P/R_{hyd}$. The hydraulic resistance of a tube, or microchannel with circular cross-section is $R_{hyd}\approx 8\mu L/\pi a^4$, where μ is the dynamic viscosity of the sample ($\mu\approx 10^{-3}$ Pa s for water), L is the length, and a is the

radius of the cross-section of the hydraulic component. Table A1 shows typical hydraulic resistances for the various tubing and microchannel.

Table S1 Hydraulic resistances.

Tube	**ϕ** µm	**2×*a*** µm	***L*** m	R_{hyd} Pa s m^{-3}
T_3 (R_3)	360	50	0.2	1.2×10^{15}
T_4 (R_4)		150	3.1	2.4×10^{14}
L_1,L_2 (R_1,R_2)		150	1.6	1.2×10^{14}
C (R_c)	-	360	0.01	2.8×10^{10}
T_5 (R_5)	700	500	0.03	1.9×10^{10}

Figure S2 shows an equivalent hydraulic circuit diagram of the hydraulic system, where R_3 is the resistance of tube T_3, R_L is the resistance of the loop L_1 and L_2, R_4 is the resistance of tube T_4 and R_c is the resistance of the microfluidic flow-cell microchannel. The volumetric flow

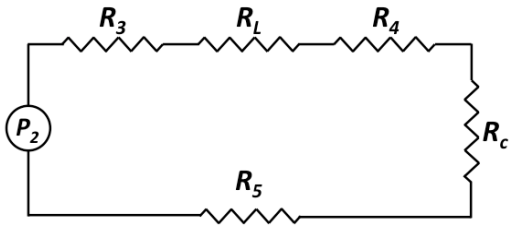

Fig. S2 Equivalent hydraulic circuit diagram.

rate is estimated with $Q\approx P_2/R_{hyd}$, where $R_{hyd}=R_3+R_L+R_4+R_c+R_5$. The average flow speed in the circular tube is estimated with $v_s\approx Q/\pi a^2$. Table A2 shows flow speed estimations for different applied pressures.

Table S2 Flow rates and flow speeds.

P_2 Bar	Q µl min^{-1}	v_s mm s^{-1}
1.0	3.75	0.61
0.5	1.88	0.31
0.3	1.16	0.19

Silicon nanowire sensor sample flowrate dependence

The silicon nanowire (Si-NW) sensors are known to be sensitive to flow rate changes due to streaming potential changes on the sensor surface (Kim et al., 2009). Figure S3 shows examples for Si-NW sensor responses to changes in the flow rate in the integrated microfluidic flow-cell. Figure S3a shows that the measured current can change by about 80% when the driving pressure is switched from P_1=1 bar to P_2=0 bar using a deionized water sample. Figure S3b shows about 14% change in current response as the driving pressure is switched from

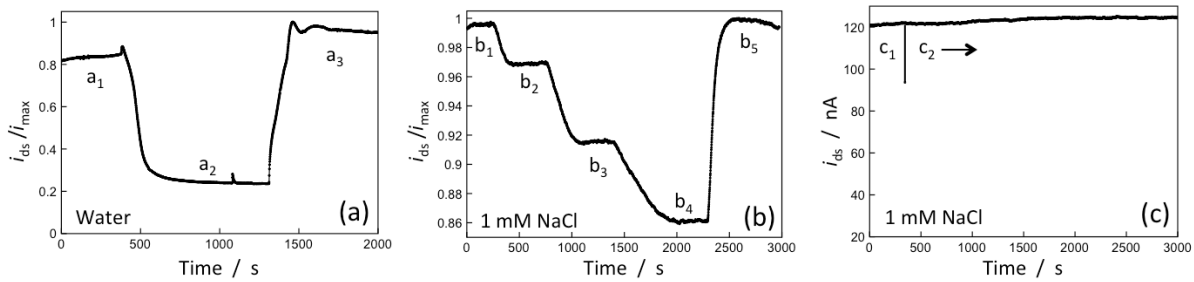

Fig. S3 Measured Si-NW sensor current to flow rate changes in a microfluidic flow-cell. (a) Deionized water flow rate change as driving pressure is changed from a_1 (P_1=1 bar) to a_2 (0 bar) and then a_3 (P_1=1 bar). (b) Flow rate of 1 mM NaCl buffer as driving pressure is changed from b_1 (P_1=1 bar) to b_2 (P_1=0.5 bar) to b_3 (P_1=0.2 bar) to b_4 (P_1=0.1 bar) and b_5 (P_1=1 bar). (c) Injector switch of 1 mM NaCl buffer from c_1 (SR_1, P_1=0.2 bar) to c_2 (SR_2, P_2=0.2 bar).

P_1=1 bar to P_1= 0.1 bar in a buffer solution containing 1 mM NaCl. These results are consistent with previous reports, i.e. decreases in the flow rate result in a decrease in conductance of p-type Si-NW devices and increased ionic strength reduces the effect of conductance changes from sample flow rate changes.[1] Figure S3c shows that flow rate changes due to sample switching can be eliminated with the automated multi-sample injection system and pressure driven flow, as described in the accompanying article.

Silicon nanowire sensor configurations

Figures S4a-c show optical microscopy images of the different device types used for experiments in this article.

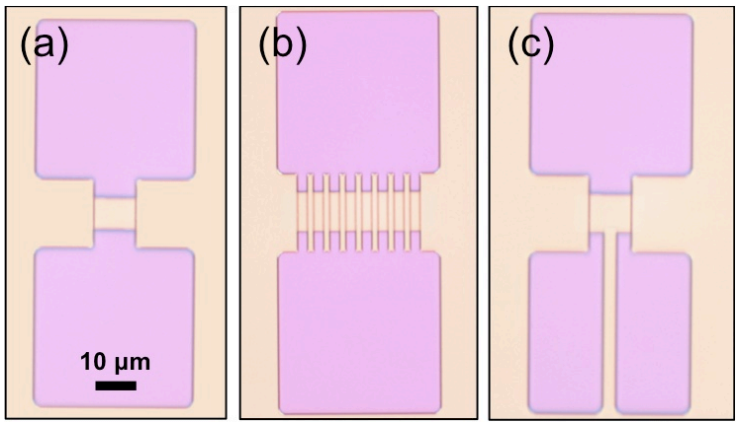

Fig. S4 Microscopy images of fabricated Si-NWs. (a) 2-wire Si-NW device. (b) 16-wire Si-NW device. (c) Differential Si-NW device with split source contact.

Silicon nanowire device physics and operation

The conductance change for Si-NWs biased in the depletion region can be approximated with $\Delta G \approx q\mu_b N_a L^{-1}\Delta\xi$, where $\Delta\xi \approx (W-(2)^{1/2}\Delta f_d)(a-(2/3)^{1/2}\Delta f_d)$ is the area of the conductance cross-section of the triangular Si-NW with width W and height a, which is modulated by a depletion length function $\Delta f_d \approx (\gamma^2 t_{ox}^2 + 2\varepsilon_{Si}\varepsilon_o(V_{fg}-\Delta V_{fb})/qN_a)^{1/2} - \gamma^2 t_{ox}^2$ with $\gamma=\varepsilon_{Si}\varepsilon_{ox}^{-1}$, where ε_{Si} and ε_{ox} are the permittivities of silicon and silicon dioxide, respectively, t_{ox} is the gate-oxide thickness, and finally the flatband voltage change is proportional to the surface potential change $\Delta V_{fb}=\zeta-\Delta\psi_o$ with $\zeta=E_{ref}-q^{-1}\phi_{Si}-Q_f C_o^{-1}-Q_{ss}C_o^{-1}+\chi^{sol}$ where E_{ref} is the reference electrode potential, $q^{-1}\phi_{Si}$ is the work function of silicon, Q_f and Q_{ss} are the fixed charge and interface states near the gate-oxide/silicon interfaces, respectively, $C_o=\varepsilon_{Si}\varepsilon_o t_{ox}^{-1}$ is the gate-oxide capacitance and χ^{sol} is the surface dipole potential of the sample solution. The flatband voltage provides a direct physical link between $\Delta\psi_o$ and ΔG. It has been assumed that the buried-oxide/silicon interface is not depleted and the back-gate is not electrostatically coupled to the front-gate, which is accomplished in practice by choosing an appropriate V_{bg}. This brief overview of the basic physical principles of the FET Si-NW sensor operation highlight a few important points that are useful to summarize: i. the application of a dual gate biasing configuration with a reference electrode in the sample buffer ensures optimal and reproducible device behavior; ii. the sensor surface should be well cleaned (e.g. short duration UV ozone) and the detrimental effects from Q_f and Q_{ss} at the gate-oxide/silicon interface minimized through thermal annealing; and iii. The contact resistance of the drain and source contacts should be minimized such that it represents a small fraction of the total quiescent sensor resistance.

Nanoscale imaging

Si-NW samples were prepared for high resolution TEM imaging by depositing a 100 nm thick silicon nitride protection layer onto the upper surface. The sample slices we prepared in a dual-beam focused ion beam (FEI Tecnai G2 F20 X-Twin FEG TEM, Maser Engineering, Enschede, The Netherlands) and transferred to a TEM imaging grid. TEM imaging (FEI 3D-Strata DB-FIB FEG, Maser Engineering, Enschede, The Netherlands) was operated at 200 kV acceleration voltage. Prior to high resolution SEM imaging the Si-NW samples were coated with a Au/Pd thin film to reduce charging of the top oxide surface. SEM imaging (LEO 1550, Zeiss) was performed at acceleration voltages ranging from 2 kV to 10 kV. A Digital Instruments Dimension 3100 AFM

was used to measure the Si-NW dimensions. All AFM images performed in tapping mode with ultra sharp (average tip diameter ~2 nm) single crystal silicon tips (SSH-NCH-10, NanoandMore, GmbH).

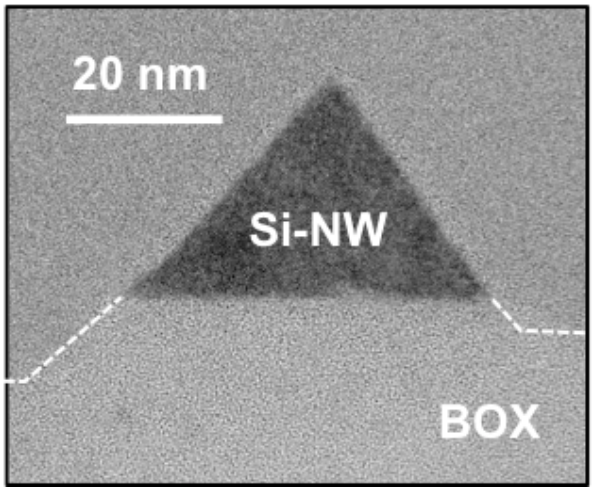

Fig. S4 High-resolution TEM Si-NW cross-section.

References

1. D.R. Kim, C.H. Lee and X.L. Zheng, *Nano Lett.*, 2009, **9**, 1984.